NJC

ROYAL SOCIETY OF CHEMISTRY

PAPER

Cite this: *New J. Chem.*, 2020, **44**, 19902

A transparent-to-gray electrochromic device based on an asymmetric viologen

Huan Ling,[ab] Hongbo Dai,[b] Fengyu Su,*[bcd] Yanqing Tian *[b] and Yan Jun Liu *[d]

Received 27th August 2020,
Accepted 20th October 2020

DOI: 10.1039/d0nj04323k

rsc.li/njc

A transparent-to-gray electrochromic device (ECD) based on an asymmetric viologen was fabricated and characterized. The core material derived from novel bipyridine salt (named 1-(2-(diethoxy-phosphoryl)ethyl)-1′-(4-vinylbenzyl)-[4,4′-bipyridine]-1,1′-diium chloride bromide, DVB) combined with complementary species of ferrocene was assembled in a device with a simple configuration of ITO/EC solution/ITO. The device was first converted to blue color from transparent when 1.0 V was applied, and then neutral gray color when the potential bias was increased to 2.0 V. Meanwhile, the corresponding optical contrasts (ΔT) were 54.5% and 22% at 392 nm and 605 nm, respectively. In addition, a good coloration efficiency of 128.9 $cm^2\ C^{-1}$ at 2.0 V and fast switching time (<2.5 s) were obtained. Finally, satisfied stability with 43.8% of ΔT (maintaining 80% of initial ΔT at 392 nm) was achieved after 2000 cyclic processes, which paves a new way to design colorless to neutral color ECDs.

1. Introduction

Electrochromism refers to the phenomenon of reversible optical switching occurring in some materials or devices upon exposure to small electrical stimuli. A large number of electrochromic materials (ECMs) have been investigated in recent decades, such as conducting polymers,[1,2] metal oxides,[3,4] metal complexes[5,6] and small organic molecules.[7–10] The ECD-based technologies have achieved extensive applications in smart windows, reflective electronics[11,12] and energy-storage devices.[13–15] Normally, ECDs can be classified into three configurations: (1) a solid structure, which is regarded as a typical sandwich model through layer-by-layer accumulation of ECMs, electrolyte and a counter electrode; (2) a solution structure, which usually consists of an EC solution of ECMs, electrolyte and a counter material in the homogeneous phase; and (3) an intermediate structure between a solid and solution structure with ECMs or ion storage materials dissolved in electrolyte.[16] Compared to the solid-structure, ECDs with solution structures are able to convert to the transparent state without extra potential bias. More importantly, it is convenient and cost-effective to prepare EC solution rather than build a complex sandwich structure.

Among EC materials, viologens (4,4′-bipyridinium dication salts) have been the subject of numerous studies owing to their superior properties including excellent stability, a clear redox mechanism and various colors.[17] Generally, viologens can be found in three states: the dicationic species (V^{2+}), radical cation ($V^{+\bullet}$), and neutral full reduced molecular state (V^0). The air-stable dicationic species (V^{2+}) can receive an electron to generate a radical cation ($V^{+\bullet}$). Remarkably, the radical cation plays a dominant role in electrochromism due to the charge transfer accompanied by valence change occurring in a nitrogen atom. The neutral fully reduced molecular V^0 was produced through another reversible reduction from the radical cation ($V^{+\bullet}$).[18] The colors of viologens could be tailored by modifying their molecular structures, and several groups have made great progress in this field.[18–20] However, developing colorless-neutral viologen-based ECDs, especially with a simple configuration and air-stable properties, still remains challenging. Thus far, Xu's group[21] and Egbert's group[21,22] adopted the method of complementary hybrid electrodes to achieve transparent-black ECDs with modified nanoporous TiO_2/viologen as the cathodic electrode and triphenylamine as the anodic electrode, but the fabrication of the ECDs required a sophisticated assembling process and strict sealing work due to the complex structure, which were incapable of matching aesthetically the surrounding environment. Up to now, there has been no report on the black/gray electrochromic phenomenon from sole symmetric substituted viologens. Recently, asymmetric viologens have attracted extensive attention for their various colors including black and gray.[17] For example, Zaera's group[23,24] demonstrated

[a] *School of Chemistry and Chemical Engineering, Harbin Institute of Technology, Harbin, 150001, China*
[b] *Department of Materials Science and Engineering, Southern University of Science and Technology, Shenzhen, 518055, China. E-mail: fysu@sustech.edu.cn, tianyq@sustech.edu.cn*
[c] *Academy for Advanced Interdisciplinary Studies, Southern University of Science and Technology, Shenzhen, 518055, China*
[d] *Department of Electrical and Electronic Engineering, Southern University of Science and Technology, Shenzhen, 518055, China. E-mail: yjliu@sustech.edu.cn*

colorless-to-black/gray based on some 1-alkyl-1′-aryl asymmetric viologens in an ion gel. The ECDs based on other asymmetric substituted viologens as the sole chromophore, such as 1-heptyl-1′-benzyl,[25] mono-heptyl[26] and 1-hexyl-1′-nonafluorohexyl[27] viologens, showed blue or magenta color. Thus, it is meaningful to explore new asymmetric viologens and study their electrochromic behaviors.

Benzyl viologen (BzV) was considered as an appropriate material utilized in the solution-type ECD,[28] but the undesired formation of radical cation dimers aggregating on electrodes will act against long-term stability. Recently, Li *et al.* developed a novel radical aryl migration of inactivated alkenes initiated by a variety of radicals such as the trifluoromethyl radical, azide radical, phosphonyl radical, sulfonyl radical and perfluoroalkyl radical,[29] and then demonstrated remote C–C bond cleavage-enabled 1,3-, 1,4-, or 1,5-vinyl migration reactions initiated by various radicals.[30] These studies suggested that there were strong interactions between the alkenyl group and free radical species. Herein, we reported the synthesis of a novel asymmetric viologen named 1-(2-(diethoxyphosphoryl)ethyl)-1′-(4-vinylbenzyl)-[4,4′-bipyridine]-1,1′-diium chloride bromide (DVB) and the performance of its corresponding ECD which was fabricated with the ITO/EC solution/ITO configuration. Introducing a styrene group would be helpful to address the aggregation problem because alkenyl will stabilize the radical cation species through the strong interactions between the viologen radical and alkenyl group. In addition, the bulk phosphate ester group would hinder the approach of intermolecular radical cations, which would be helpful to restrain the aggregation behaviors of viologen radicals.[28] The DVB-based simple solution-type ECD showed transparent-blue-gray colors at different voltages and excellent electrochromic performance (Scheme 1).

2. Experimental section

2.1 Materials and instruments

Commercially available raw chemicals were used without further purification. 4,4′-Bipyridine was purchased from J&K Chemical (Beijing, China). 2-Bromoethylphosphonate and 4-chloromethyl styrene were ordered from Energy Chemical (Shanghai, China). 1-(chloromethyl)-4-vinylbenzene was purchased from Aladdin (Shanghai, China). All solvents were purchased from XiLong Scientific (Guangzhou, China). ITO glasses were purchased from NSG Group (Osaka, Japan).

Nuclear magnetic resonance (NMR) spectra were acquired through NMR (Bruker 400M; 400 MHz for ^{1}H NMR, 101 MHz for ^{13}C NMR, Bremen). Mass spectra were obtained using an HRMS (Q-Exactive, Massachusetts). The electrochemical properties were evaluated using an electrochemical workstation (Ametek Parstat 3000A-DX, Berwyn). The optical properties were measured using a UV-vis spectrophotometer (L6020365, Waltham) and Colorimeter (CHN Spec CS-820, Guangzhou) combined with a Function/Arbitrary Waveform Generator (Rigol DG4102, Suzhou). A digital camera was used to record the photographs of the device.

2.2 Materials' synthesis

Compound **B** was synthesized according to the published literature.[31] Firstly, 4,4′-bipyridine (**A**, 3 g, 19 mmol) and diethyl bromoethyl phosphonate (4.64 g, 19 mmol) were added to a 100 ml round-bottomed flask and then, 30 ml acetone was injected into the flask. The reaction mixture was heated to 50 °C and stirred until a solid precipitate of mono-quaternary ammonium salt was formed. Subsequently, the precipitate was filtered and the filtrate was heated to 50 °C again until no more solid of mono-cation salts formed. Finally, the precipitate was washed with ether and dried over under vacuum to give a pale yellow product 1-(2-(diethoxyphosphoryl)ethyl)-[4,4′-bipyridin]-1-ium bromide (compound **B**, 3.4 g, 8.5 mmol) with yield of 45%. ^{1}H NMR (400 MHz, D_2O) δ 9.39 (d, J = 6.5 Hz, 2H), 8.85 (s, 2H), 8.73 (d, J = 6.8 Hz, 2H), 8.12 (s, 2H), 4.90 (dt, J = 14.1, 7.4 Hz, 2H), 4.09–3.91 (m, 4H), 2.86–2.66 (m, 2H), 1.17 (q, J = 6.8 Hz, 6H).

The mixture of compound **B** (0.65 g, 1.6 mmol) and 1-(chloromethyl)-4-vinylbenzene (0.3 g, 1.97 mmol) in CH_3CN (25 ml) was heated to 60 °C for 72 h. The resulting solution was concentrated under reduced pressures after cooling down to room temperature. And then, the mixture was purified with fresh silica column chromatography to give a yellow product 1-(2-(diethoxyphosphoryl)ethyl)-1′-(4-vinylbenzyl)-[4,4′-bipyridine]-1,1′-diium chloride bromide (DVB, 0.34 g, 0.62 mmol) with a yield of 39%. ^{1}H NMR (400 MHz, D_2O) δ 9.10 (dd, J = 11.4, 7.1 Hz, 4H), 8.49 (dd, J = 16.0, 7.0 Hz, 4H), 7.50 (d, J = 8.3 Hz, 2H), 7.41 (d, J = 8.3 Hz, 2H), 6.70 (dd, J = 17.7, 11.0 Hz, 1H), 5.80 (d, J = 16.7 Hz, 3H), 5.28 (d, J = 11.5 Hz, 1H), 4.95 (dt, J = 16.5, 7.2 Hz, 2H), 4.05 (dq, J = 8.2, 7.1 Hz, 4H), 2.73 (dt, J = 18.5, 7.2 Hz, 2H), 1.17 (t, J = 7.1 Hz, 6H). ^{13}C NMR (101 MHz, D2O) δ 150.72, 150.12, 145.92, 145.53, 139.18, 135.71, 131.54, 129.69, 127.22, 127.09, 115.94, 64.56, 63.95, 55.88, 26.68, 25.27, 15.52. HRMS m/z calcd for $C_{25}H_{31}N_2O_3P^{2+}$ ($[M]^{2+}$) 219.1031, found 219.1029.

2.3 Fabrication of ECDs

First, small frame shape spacers were put on the edges of an ITO glass and served as a gasket; and then another ITO glass was placed on top of this ITO glass. The two ITO glasses were

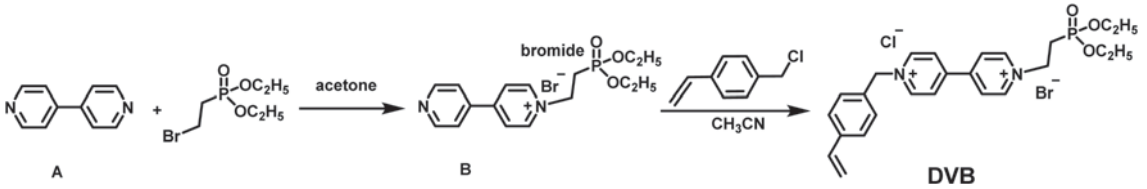

Scheme 1 Synthetic route of DVB.

pressed together tightly through a subpress, leaving a 70 μm gap distance. The EC solution containing 0.01 M viologen and 0.03 M ferrocene in propylene carbonate was injected into the gap without strict sealing.

3. Results and discussion

A two-electrode system was utilized to characterize the electrochemical properties of ECDs. The detected peaks at −0.11 V/0.11 V were the redox couple of Fc/Fc^{+}. With an increase in the applied voltage, the dicationic species of DVB^{2+} was reduced to the radical cation $DVB^{+\bullet}$ with single electron exchange. The corresponding cathodic and anodic peaks were at −0.99 V/−0.59 V.

Simultaneously, the color of the ECD changed to blue from light yellow transparent (yellow due to the dissolution of ferrocene) when 1.0 V potential was applied as depicted in Fig. 1b. The redox peaks at −1.55 V/−1.13 V would be the reversible transformation of $DVB^{0}/DVB^{+\bullet}$. Therefore, we assumed that the ECD possessed a similar mechanism compared with other typical viologens although the EC solution was exposed to moisture.[32] At the same time, the ECD gradually exhibited bluish gray color upon imposing 1.8 V potential and completely gray at 2.0 V.

In order to understand the effect on the electron distribution of asymmetric viologen, the energy level including the HOMO (highest occupied molecular orbital) and LUMO (lowest unoccupied molecular orbital) diagrams of DVB^{2+}, two kinds of $DVB^{+\bullet}$ and DVB^{0} were obtained by the density functional theory (DFT) calculations as shown in Fig. 2. The HOMO and LUMO were calculated as −11.43 eV and −9.34 eV respectively. Two available radical cations generated in the first reduced state. And the HOMO (−7.08 eV) and LUMO (−4.00 eV) for two possible radical cations were identical, which indicated that they possess the same probability produced from dications. The HOMO (−3.07 eV) and LUMO (−0.15 eV) levels of the fully reduced species of DVB were further increased.

Fig. 3a presents the UV-vis spectra of a DVB-based ECD with increasing voltages. High transparency was detected at 0 V with the transmittance approximately 75% from 380 nm to 800 nm. Blue color appeared at 1.0 V and didn't turn to deeper until 1.5 V was reached, which could be attributed to the high concentration of $DVB^{+\bullet}$. Simultaneously, the peaks at 392 nm and 605 nm emerged. With the potential increased, part of $DVB^{+\bullet}$ was reduced to DVB^{0} triggered by sufficient ferrocene. As a result, decreased absorption at 605 nm was detected, but not at 392 nm.

The stability and response time were two fundamental parameters for the ECD, and were evaluated at 392 nm where the largest ΔT (optical contrast) was obtained in this work.

As shown in Fig. 3b, the original transmittances were 72.9% for the bleached state and 20.1% for the colored state, and ΔT was calculated as 52.8%. Slightly increased ΔT (54.5%) was obtained after dozens of cycles. With the ECD runs, no obvious change occurred for bleaching transmittance (T_b), which indicated that the radical cation species of DVB didn't substantially aggregate on the electrodes. The prevention of the side aggregation process would be attributed to the addition of ferrocene[33] and the difficulty in the formation of radical dimers. As a result, 43.8% of ΔT remained after 2000 cyclic processes, which was better than those of some reported viologen-based liquid ECDs with strict sealing.[34] The overuse of ferrocene and relatively low concentration of viologen would speed up the redox reactions and diffusion process. Therefore, the response times were calculated to be 2.2 s and 1.9 s for coloring and bleaching respectively as depicted in Fig. 3c, which were faster than most of the reported viologen-based gel-type ECDs.[35] A feasible assumption was proposed to account for the superior properties of DVB-based ECDs as shown in Fig. 4. First, light blue color appeared when the radical cation species was generated. From the results of Fig. 1a and Fig. 3a, no obvious peaks of radical dimers were observed, indicating that the radicals are free.

Then, the free radical species was captured by the alkenyl group and the distribution of electron clouds were changed, which would lead to the generation of extended-conjugation viologen intermediate species. This extended-conjugation viologen intermediate species not only could stabilize $DVB^{+\bullet}$ but

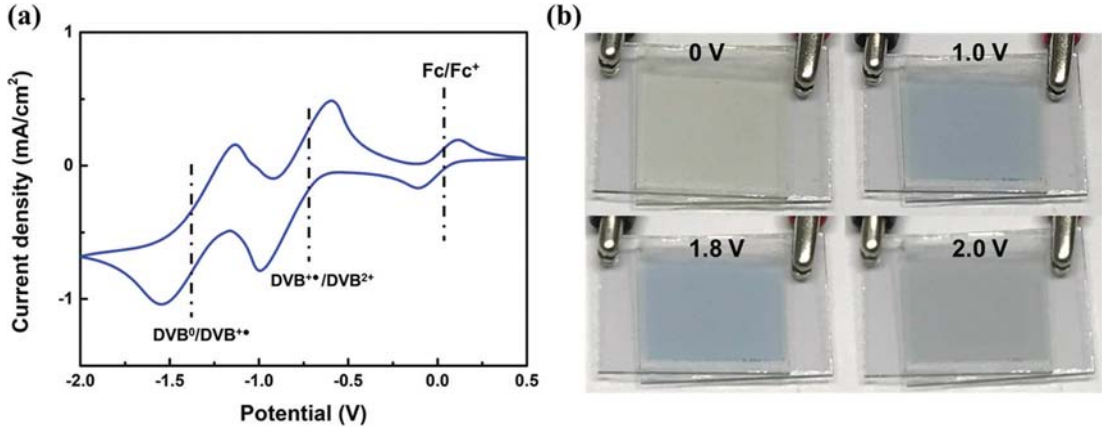

Fig. 1 (a) CV curve of an ECD at a scan rate of 100 mV s^{-1} and (b) photographs of the ECD under different potential biases.

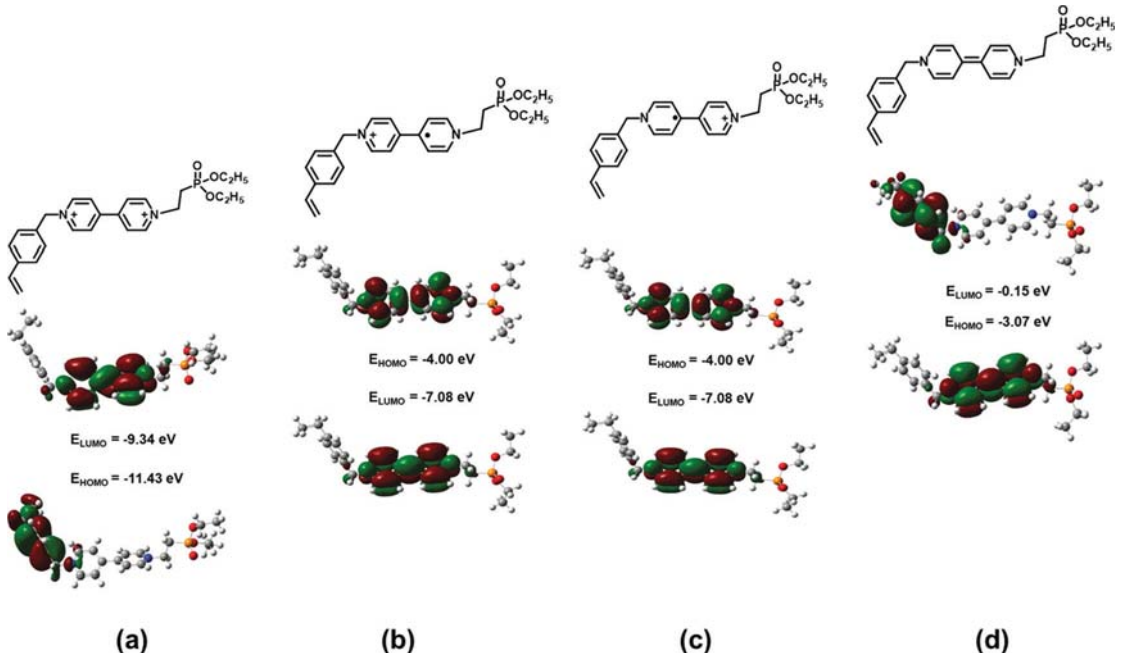

Fig. 2 Frontier molecular orbitals of DVB obtained from DFT calculation through Gaussian 09: (a) dication state, (b) radical cation state ((diethoxyphosphoryl)ethyl side), (c) radical cation state (vinylbenzyl side), and (d) full reduced state.

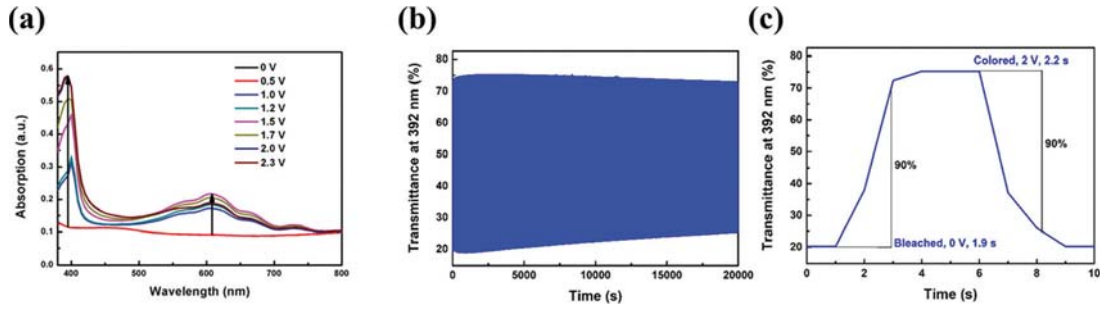

Fig. 3 (a) UV-vis absorption of the ECD under different potential biases, (b) switching curves at a potential of 2.0 V (colored time for 5 s) and 0 V (bleached time for 5 s) for 2000 cyclic processes, and (c) calculated coloring and bleaching time with an applied potential of 2.0 V (colored) and 0 V (bleached).

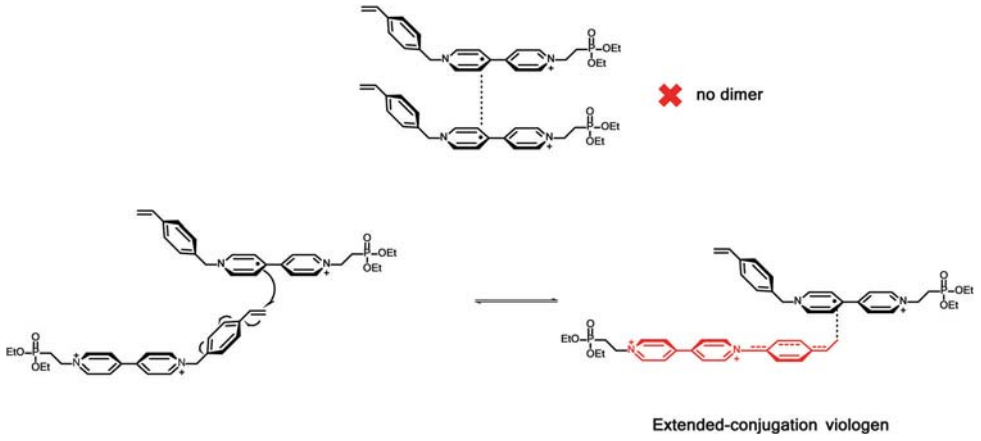

Fig. 4 Proposed intermolecular interactions between viologens.

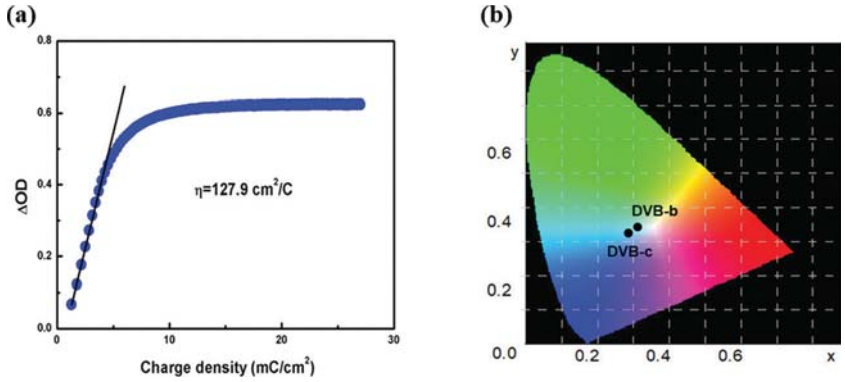

Fig. 5 (a) Optical density *versus* charge density at 392 nm and (b) colorimetry of ECDs in the colored and bleached states.

Table 1 Colorimetric parameters for DVB-based ECDs in different redox states

Redox states for ECD	L*	a*	b*
DVB-b[a]	85.72	−3.55	2.18
DVB-c[b]	63.78	−6.61	−2.18

[a] b represents the bleached state (0 V). [b] c represents the colored state (2.0 V).

also offer the feature of neutral-chromophore because 1-alkyl-1′-aryl substituted viologens generated a similar extended-conjugation structure and showed black or gray in the colored state.[23,24] The driving force for the creation of extended-conjugation viologen was the emergence of a stable larger delocalization system and the strong reactive tendency between free radical species and the terminal alkenyl group aforementioned. Particularly, gray color maintained in the colored state in air, as far as we know, was the first reported air-stable transparent-gray ECD.

The coloration efficiency (CE) was another important parameter to estimate the performance of ECDs, generally, it is defined as follows:

$$\mathrm{CE} = \eta = \Delta\mathrm{OD}/\Delta Q = \log\left(T_\mathrm{b} - T_\mathrm{c}\right)/\Delta Q$$

where T_b and T_c represent the transmittance in bleached and colored states respectively, and ΔQ is the injected charge density (CD) corresponding to the optical contrast. The value of CE was calculated from the linear region of the ΔQ-CD from Fig. 5a. The value of 127.9 $\mathrm{cm}^2\ \mathrm{C}^{-1}$ at 392 nm and 2.0 V was satisfactory, which suggested that the DVB-based ECD possessed the potential ability to modulate ultraviolet light with visual color change. The CIE system was constantly utilized to characterize the chromaticity values with three main parameters comprising of L*, a* and b*. L* represents lightness, and a* and b* were used to describe the green–red and blue–yellow color constituents. As depicted in Table 1, the decrease from 85.72 to 63.78 revealed the transformation from the transparent to colored state, simultaneously, neutral grayish color was observed ($|a^*|$ and $|b^*| < 10$), which matched well with the color appearance at 2.0 V as shown in Fig. 1b. Fig. 5b shows the colorimetry diagram of ECDs in the colored and bleached states.

4. Conclusions

In this work, an air-stable transparent-gray liquid ECD based on an asymmetric viologen and simple device structure (ITO/EC solution/ITO) was successfully developed. The transparent-gray behavior was achieved through the synthesized 1-alkyl-1′-vinylbenzyl substituted viologen. In addition, fast response time (<2.5 s), satisfactory stability (43.8% maintained after 5000 s cycling time) were obtained with the EC solution exposed to air. Finally, the ECD showed some advantages compared with the reported colorless-black/gray ECDs, such as simple configuration, easy fabrication, good compatibility with the surrounding environment and competitive response time, which paves a new way to develop low-cost transparent-gray ECDs.

Conflicts of interest

There are no conflicts of interest to declare.

Acknowledgements

The authors would like to thank Shenzhen fundamental research programs (JCYJ20170412152922553, JCYJ20170817111349280 and JCYJ20180305180635082), the start-up fund of SUSTech (Y01256114), and the high-level university construction fund for SUSTech (G01256018).

References

1 T. Abidin, Q. Zhang, K.-L. Wang and D.-J. Liaw, *Polymer*, 2014, **55**, 5293–5304.
2 A. Chaudhary, D. K. Pathak, S. Mishra, P. Yogi, P. R. Sagdeo and R. Kumar, *Sol. Energy Mater. Sol. Cells*, 2018, **188**, 249–254.
3 V. V. Kondalkar, R. R. Kharade, S. S. Mali, R. M. Mane, P. B. Patil, P. S. Patil, S. Choudhury and P. N. Bhosale, *Superlattices Microstruct.*, 2014, **73**, 290–295.
4 H. Gu, C. Guo, S. Zhang, L. Bi, T. Li, T. Sun and S. Liu, *ACS Nano*, 2018, **12**, 559–567.

5 N. Elool Dov, S. Shankar, D. Cohen, T. Bendikov, K. Rechav, L. J. W. Shimon, M. Lahav and M. E. van der Boom, *J. Am. Chem. Soc.*, 2017, **139**, 11471–11481.

6 K. Hoshino, M. Okuma and K. Terashima, *J. Phys. Chem. C*, 2018, **122**, 22577–22587.

7 L. Ji, Y. Dai, S. Yan, X. Lv, C. Su, L. Xu, Y. Lv, M. Ouyang, Z. Chen and C. Zhang, *Sci. Rep.*, 2016, **6**, 30068.

8 S. Nachimuthu, W. R. Shie, D. J. Liaw, R. V. Romashko and J. C. Jiang, *J. Phys. Chem. B*, 2019, **123**, 4735–4744.

9 M. Walesa-Chorab and W. G. Skene, *ACS Appl. Mater. Interfaces*, 2017, **9**, 21524–21531.

10 D. Weng, Y. Shi, J. Zheng and C. Xu, *Org. Electron.*, 2016, **34**, 139–145.

11 L. M. N. Assis, L. Ponez, A. Januszko, K. Grudzinski and A. Pawlicka, *Electrochim. Acta*, 2013, **111**, 299–304.

12 F. Sentanin, R. C. Sabadini, S. C. Barros, W. R. Caliman, C. C. S. Cavalheiro, J. Kanicki, J. P. Donoso, C. J. Magon, I. D. A. Silva, M. M. Silva and A. Pawlicka, *Electrochim. Acta*, 2019, **301**, 174–182.

13 T. G. Yun, D. Kim, Y. H. Kim, M. Park, S. Hyun and S. M. Han, *Adv. Mater.*, 2017, **29**, 1606728.

14 T. Y. Yun, X. Li, S. H. Kim and H. C. Moon, *ACS Appl. Mater. Interfaces*, 2018, **10**, 43993–43999.

15 P. Zhang, F. Zhu, F. Wang, J. Wang, R. Dong, X. Zhuang, O. G. Schmidt and X. Feng, *Adv. Mater.*, 2017, **29**, 1604491.

16 J. W. Kim and J. M. Myoung, *Adv. Funct. Mater.*, 2019, **29**, 1808911.

17 K. Madasamy, D. Velayutham, V. Suryanarayanan, M. Kathiresan and K.-C. Ho, *J. Mater. Chem. C*, 2019, **7**, 4622–4637.

18 S.-Y. Kao, Y. Kawahara, S. i. Nakatsuji and K.-C. Ho, *J. Mater. Chem. C*, 2015, **3**, 3266–3272.

19 Y. Alesanco, A. Vinuales, J. Palenzuela, I. Odriozola, G. Cabanero, J. Rodriguez and R. Tena-Zaera, *ACS Appl. Mater. Interfaces*, 2016, **8**, 14795–14801.

20 Y. Alesanco, A. Viñuales, J. Ugalde, E. Azaceta, G. Cabañero, J. Rodriguez and R. Tena-Zaera, *Sol. Energy Mater. Sol. Cells*, 2018, **177**, 110–119.

21 M. Li, Y. Wei, J. Zheng, D. Zhu and C. Xu, *Org. Electron.*, 2014, **15**, 428–434.

22 C. Kortz, A. Hein, M. Ciobanu, L. Walder and E. Oesterschulze, *Nat. Commun.*, 2019, **10**, 4874.

23 Y. Alesanco, A. Vinuales, G. Cabanero, J. Rodriguez and R. Tena-Zaera, *ACS Appl. Mater. Interfaces*, 2016, **8**, 29619–29627.

24 Y. Alesanco, A. Viñuales, G. Cabañero, J. Rodriguez and R. Tena-Zaera, *Adv. Opt. Mater.*, 2017, **5**, 1600989.

25 M. Kim, Y. M. Kim and H. C. Moon, *RSC Adv.*, 2020, **10**, 394–401.

26 H. Oh, D. G. Seo, T. Y. Yun, C. Y. Kim and H. C. Moon, *ACS Appl. Mater. Interfaces*, 2017, **9**, 7658–7665.

27 G. K. Pande, N. Kim, J. H. Choi, G. Balamurugan, H. C. Moon and J. S. Park, *Sol. Energy Mater. Sol. Cells*, 2019, **197**, 25–31.

28 H.-F. Yu, K.-I. Chen, M.-H. Yeh and K.-C. Ho, *Sol. Energy Mater. Sol. Cells*, 2019, **200**, 110020.

29 L. Li, Z. L. Li, F. L. Wang, Z. Guo, Y. F. Cheng, N. Wang, X. W. Dong, C. Fang, J. Liu, C. Hou, B. Tan and X. Y. Liu, *Nat. Commun.*, 2016, **7**, 13852.

30 L. Li, Z.-L. Li, Q.-S. Gu, N. Wang and X.-Y. Liu, *Sci. Adv.*, 2017, **3**, e1701487.

31 Y. Rong, S. Kim, F. Su, D. Myers and M. Taya, *Electrochim. Acta*, 2011, **56**, 6230–6236.

32 B. Gelinas, D. Das and D. Rochefort, *ACS Appl. Mater. Interfaces*, 2017, **9**, 28726–28736.

33 H.-C. Lu, S.-Y. Kao, T.-H. Chang, C.-W. Kung and K.-C. Ho, *Sol. Energy Mater. Sol. Cells*, 2016, **147**, 75–84.

34 C.-R. Zhu, J.-F. Long, Q. Tang, C.-B. Gong and X.-K. Fu, *J. Appl. Electrochem.*, 2018, **48**, 1121–1129.

35 Y. Alesanco, A. Vinuales, J. Rodriguez and R. Tena-Zaera, *Materials*, 2018, 11, 414.